



# Technical and economic feasibility study of high-current HTS bus bars for fusion reactors

Roberto Guarino<sup>\*</sup>, Rainer Wesche, Kamil Sedlak

École Polytechnique Fédérale de Lausanne (EPFL), Swiss Plasma Center (SPC), CH-5232 Villigen PSI, Switzerland

## ARTICLE INFO

### Keywords:

HTS  
Power cables  
Feasibility study  
Economic analysis  
Fusion reactors

## ABSTRACT

In this study, we present a technical and economic assessment of high-current HTS bus bars for primary use in fusion reactors. Our objective is to verify the technical feasibility of such conductors and, for this purpose, we carry out a conceptual design of 66 and 105 kA DC bus bars, e.g. as a potential solution for powering the European DEMO power plant. We employ commercial HTS tapes and reasonable (as well as conservative) assumptions on cooling configurations and costs. Then, we compute the material, manufacturing and operating costs of these bus bars, comparing them with conventional (i.e. Al) conductors. Different Al current densities are considered, showing their impact on the total costs and on their technical feasibility. The cumulative operating costs over a 30-year period, based on nowadays realistic values for electricity cost and discount rate, are then briefly compared and discussed. We believe the present work could be of interest in designing the power supply system of future fusion reactors and other high-current industrial applications.

## 1. Introduction

The use of high-temperature superconductors (HTS) in power transmission lines has gained a growing interest above all for their superior efficiency compared to conventional conductors. Therefore, several recent projects worldwide have demonstrated the successful application of HTS cables in power grids and substations [1–11].

A few research studies have been focused on the economic assessment of HTS cables, and, in particular, on their competitiveness with respect to conventional conductors. In general, the results have shown that operating HTS cables at LN<sub>2</sub> temperatures is not always convenient with respect to conventional (i.e. Al or Cu) cables, especially if short line lengths and critical current densities below 10<sup>6</sup> kA m<sup>-2</sup> are considered [12,13]. Other authors, besides reducing the operating costs thanks to reduced power losses, have emphasised that HTS power transmission lines have the additional advantage of allowing lower voltage levels, thus bringing economic benefits also to auxiliary devices such as transformers and power switches [14,15].

In recent years, the improvement in the manufacturing technologies of HTS wires and tapes has allowed to reach larger critical currents. This has progressively decreased the HTS material costs (strictly speaking, their operating cost per unit length, measured in \$ kA<sup>-1</sup> m<sup>-1</sup>), making them more and more attractive for replacing conventional conductors

[16].

Another point to be considered is the application cases that have been studied in the literature. The works mentioned above, in most of the cases, refer to HTS conductors for high-voltage and/or AC power grid applications, usually with small current ratings (e.g., in the order of few kA). Nevertheless, some industrial applications operate at lower voltage levels and larger currents, thus they could potentially benefit from an HTS-based solution. It is the case, for instance, of tokamaks for plasma and fusion energy research, such as the International Thermonuclear Experimental Reactor (ITER), the Japan Torus (JT)-60, and the European Demonstration Fusion Power Plant (DEMO). The operating currents of the superconducting magnets in these projects are in the range 20–70 kA, depending on the coil type and material, and on the considered plasma scenario [17–20], and suitable power supplies have been or are being developed. Recent studies, targeted at reducing the voltage to ground of the European DEMO toroidal field coils, foresee possible operating currents of 100 kA and beyond [21]. In ITER, water-cooled Al bus bars are proposed for connecting the superconducting magnets to the corresponding power supply systems [22].

In this study, we focus on high-current bus bars for primary use in fusion reactors, for which we evaluate the possible use of HTS cables instead of conventional Al bus bars. The objective of the present study is twofold. On one side, a preliminary conceptual design of high-current

<sup>\*</sup> Corresponding author.

E-mail address: [roberto.guarino@epfl.ch](mailto:roberto.guarino@epfl.ch) (R. Guarino).

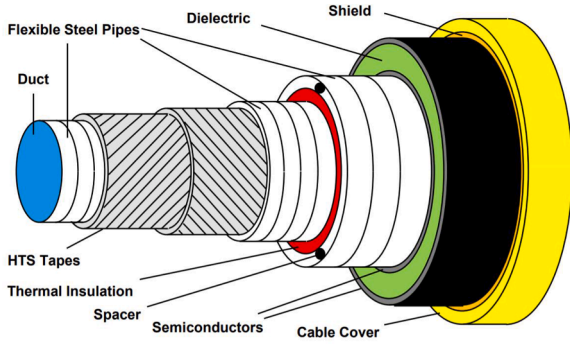


Fig. 1. Schematic cross section of a single-phase HTS power cable with warm dielectric (example case for  $N = 2$ ).

HTS bus bars is presented, considering two representative values of the operating current, i.e. 66 and 105 kA. The second objective is to assess the economic feasibility of the designed HTS bus bars, considering material, manufacturing and operating costs, and making use of conservative assumptions.

Our results could be of interest not only for the design of bus bars and power supply systems for future fusion reactors, but also for other high-current applications (e.g. in aluminium electrolysis plants [23]), despite the need of dedicated cryogenic equipment and additional components might lead to larger investment and/or maintenance costs.

## 2. Cable design

### 2.1. HTS bus bars

In the present work, we consider DC HTS power cables with a warm dielectric, whose schematic view is shown in Fig. 1. Essentially, HTS tapes are wound in an even number of layers around a flexible stainless steel former, and are then enveloped by a flexible cryostat, usually made of corrugated stainless steel pipes with interposed thermal insulation. Outside of the cryostat, a conventional dielectric and an outer electromagnetic shield are present.

The HTS tapes are wound with a certain twist angle  $\varphi$  with respect to the axis of the flexible former, and are arranged in opposite directions over an even number of layers  $N$ . The number of tapes per layer is computed as:

$$n = \frac{2\pi r_o}{w} \cos\varphi \quad (1)$$

where  $r_o$  is the outer radius of the flexible former and  $w$  the tape width. Note that, for a large number of layers, a variation of  $\varphi$  from layer to layer is required to ensure a uniform current distribution (see, e.g., Ref. [24] for details). For the purpose of the present study, here we do not deepen further these constructive details. We present only a conceptual design of the HTS bus bars with an overestimated number of tapes, thus pursuing a conservative analysis also from the economic point of view.

Neglecting the background magnetic field generated by the second bus bar of each pair, the HTS tapes are subjected only to a field component tangential to their wide faces, i.e. the self-field of the multi-layer conductor:

$$B_s = \frac{\mu_0}{2\pi(r_o + Nt)} I_{op} = \frac{\mu_0}{2\pi(r_o + Nt)} n N I_{tape} \quad (2)$$

where  $\mu_0 = 4\pi \cdot 10^{-7} \text{H m}^{-1}$  is the magnetic permeability of vacuum,  $t$  the tape thickness,  $I_{op}$  the operating current of the cable and  $I_{tape}$  the average current in each HTS tape.

For a given value of the magnetic field  $B_s$  and of the operating temperature  $T_{op}$ , there is only one possible value of the HTS tape critical

current  $I_{c,tape}$ , which corresponds to a bus bar critical current:

$$I_c = n N I_{c,tape}(B_s, T_{op}) \quad (3)$$

Finally, the intersections of the load lines described by the inverse of Eq. (2) with the  $I_{c,tape}(B_s, T_{op})$  curves provides the tape critical current for a given number of layers (see Fig. A1 in Appendix for details on the graphical procedure).

In DC power cables, the heat leak through the thermal insulation is the only component of the power losses of interest, and its value per unit length is given by [25]:

$$P_{th} = \frac{2\pi k}{\ln \frac{r_{th,o}}{r_{th,i}}} (T_{amb} - T_{op}) \quad (4)$$

where  $k$  is the thermal conductivity of the thermal insulation,  $T_{amb}$  the ambient temperature and  $r_{th,i}$  and  $r_{th,o}$  the outer and the inner radii of the thermal insulation, respectively. The total power to be considered for computing the operating costs corresponds to the refrigeration (or cooling) power [25]:

$$P_{HTS} = \frac{1}{\eta} \frac{T_{amb} - T_{op}}{T_{op}} P_{th} \quad (5)$$

where  $\eta$  is the cryo-plant efficiency. In Eq. (5), the ratio  $\frac{T_{amb} - T_{op}}{T_{op}}$  is the inverse Carnot efficiency, while  $\frac{1}{\eta}$  represents the coefficient of performance of the cryo-plant.

### 2.2. Al bus bars

Here we consider Al bus bars as conventional conductors. The required cross section is given by:

$$A_{Al} = \frac{I_{op}}{J_{Al}} \quad (6)$$

The total electric power losses, in this case, are due to Joule heating and their value per unit length of the bus bar is given by:

$$P_{Al} \approx \rho_{Al} J_{Al} I_{op} \quad (7)$$

where the assumed operating temperature must be specified in order to evaluate the electrical resistivity  $\rho_{Al}$ .

## 3. Economic analysis

### 3.1. Infrastructure costs

In the following, we denote with infrastructure costs the sum of the material and manufacturing costs for the realisation of the considered bus bars. We neglect all the costs associated with ancillary structures, e.g. cryo-plant, water-cooling circuit, etc., which depend on many other system-related choices and cannot be estimated from scratch.

The material cost of HTS cables is given by:

$$C_{HTS,mat} = n N C_{HTS} \quad (8)$$

where  $C_{HTS,mat}$  is the total material cost per unit length and  $C_{HTS}$  the cost of one HTS tape per unit length and can be eventually related to the operating conditions ( $B_s$  and  $T_{op}$ ) through:

$$\tilde{C}_{HTS} = \frac{C_{HTS}}{I_{tape}} \quad (9)$$

which is measured in  $\$ \text{kA}^{-1} \text{m}^{-1}$ .

The material cost of conventional conductors, instead, can be taken proportional to the weight, i.e.:

$$C_{Al,mat} = d_{Al} A_{Al} C_{Al} \quad (10)$$

**Table 1**

66 kA HTS bus bar design based on three possible operating temperatures and four possible outer radii of the flexible former.

$T_{op} = 50$ K (He gas cooling)					
		$r_o = 25.0$ mm	$r_o = 40.0$ mm	$r_o = 55.0$ mm	$r_o = 70.0$ mm
$N$	–	34	54	74	95
$N$	–	8	4	4	2
$nN$	–	272	216	296	190
$B$	T	0.666	0.402	0.401	0.236
$I_{tape}$	A	242.6	305.6	223.0	347.4
$I_{c,tape}$	A	315.8	375.9	375.2	435.9
$I_c$	kA	85.9	81.2	111.1	82.8
$I_{op}/I_c$	%	76.8	81.3	59.4	79.7
$T_{op} = 65$ K (He gas cooling)					
		$r_o = 25.0$ mm	$r_o = 40.0$ mm	$r_o = 55.0$ mm	$r_o = 70.0$ mm
$N$	–	34	54	74	95
$N$	–	16	8	6	4
$nN$	–	544	432	444	380
$B$	T	0.631	0.390	0.313	0.234
$I_{tape}$	A	121.3	152.8	148.6	173.7
$I_{c,tape}$	A	154.2	184.1	195.9	216.7
$I_c$	kA	83.9	79.5	87.0	82.3
$I_{op}/I_c$	%	78.7	83.0	75.9	80.2
$T_{op} = 77.5$ K (LN <sub>2</sub> cooling)					
		$r_o = 25.0$ mm	$r_o = 40.0$ mm	$r_o = 55.0$ mm	$r_o = 70.0$ mm
$N$	–	34	54	74	95
$N$	–	42	22	14	10
$nN$	–	1428	1188	1036	950
$B$	T	0.566	0.406	0.304	0.248
$I_{tape}$	A	46.2	55.6	63.7	69.5
$I_{c,tape}$	A	57.8	72.1	82.7	92.6
$I_c$	kA	82.5	85.7	85.7	88.0
$I_{op}/I_c$	%	77.5	77.0	77.0	75.0

**Table 2**

105 kA HTS bus bar design based on three possible operating temperatures and four possible outer radii of the flexible former.

$T_{op} = 50$ K (He gas cooling)					
		$r_o = 25.0$ mm	$r_o = 40.0$ mm	$r_o = 55.0$ mm	$r_o = 70.0$ mm
$N$	–	34	54	74	95
$N$	–	14	8	6	4
$nN$	–	476	432	444	380
$B$	T	1.000	0.667	0.541	0.404
$I_{tape}$	A	138.7	243.1	236.5	276.3
$I_{c,tape}$	A	277.3	314.9	338.7	374.2
$I_c$	kA	132.0	136.0	150.4	142.2
$I_{op}/I_c$	%	79.6	77.2	69.8	73.8
$T_{op} = 65$ K (He gas cooling)					
		$r_o = 25.0$ mm	$r_o = 40.0$ mm	$r_o = 55.0$ mm	$r_o = 70.0$ mm
$N$	–	34	54	74	95
$N$	–	30	16	10	8
$nN$	–	1020	864	740	760
$B$	T	0.948	0.639	0.459	0.394
$I_{tape}$	A	102.9	121.5	141.9	138.2
$I_{c,tape}$	A	130.1	153.8	173.6	183.5
$I_c$	kA	132.7	132.9	128.5	139.5
$I_{op}/I_c$	%	79.1	79.0	81.7	75.3
$T_{op} = 77.5$ K (LN <sub>2</sub> cooling)					
		$r_o = 25.0$ mm	$r_o = 40.0$ mm	$r_o = 55.0$ mm	$r_o = 70.0$ mm
$N$	–	34	54	74	95
$N$	–	76	36	26	18
$nN$	–	2584	1944	1924	1710
$B$	T	0.753	0.534	0.450	0.364
$I_{tape}$	A	25.5	54.0	54.6	61.4
$I_{c,tape}$	A	47.4	69.8	67.3	76.4
$I_c$	kA	122.5	135.7	129.5	130.6
$I_{op}/I_c$	%	85.7	77.4	81.1	80.4

where  $C_{Al,mat}$  is the total material cost per unit length,  $d_{Al}$  the Al material density and  $C_{Al}$  the Al cost per unit weight.

Finally, the total infrastructure cost per unit bus bar length is defined as follows:

$$C_{i,inf} = C_{i,mat} + C_{i,mfg} \quad (11)$$

where  $C_{i,mfg}$  refers to the manufacturing costs and  $i$  to HTS or Al.

### 3.2. Operating costs

While the infrastructure costs are assumed to incur only at the beginning of the investment period (i.e., at the year 0), the operating costs incur every year and the corresponding (negative) cash flow must be discounted. The discount rate at the year  $j$  is given by:

$$\xi_j = \frac{(1+p)^{j-1}}{(1+q)^j} \quad (12)$$

where  $p$  is the inflation rate and  $q$  the interest rate. Therefore, the total operating costs in  $M$  years for the HTS and the Al solution are given, respectively, by:

$$C_{HTS,op,tot} = \sum_{j=1}^M C_{HTS,op,j} = \sum_{j=1}^M \xi_j (e\tau P_{HTS} + C_{HTS,mnt,j}) \quad (13a)$$

$$C_{Al,op,tot} = \sum_{j=1}^M C_{Al,op,j} = \sum_{j=1}^M \xi_j e\tau P_{Al} \quad (13b)$$

where  $e$  is the electricity price,  $\tau$  the total number of hours per year and  $f$  the duty cycle. Note that, while in the case of conventional bus bars the duty cycle can follow exactly that of the superconducting magnets, it would be not convenient to warm up the HTS bus bars for short durations, thus the required room-temperature refrigerating power  $P_{HTS}$  must be accounted for the whole time except the hours needed for maintenance. In Eq. (13a), in fact, we have inserted also an additional maintenance cost of the cryo-plant  $C_{HTS,mnt}$  which adds to the yearly operating costs and is not considered for conventional bus bars. Since in fusion reactor the cryo-plant maintenance must anyway take place, we expect that the bus bars share only a small fraction of the total cryo-plant maintenance costs.

Note also that we neglect the additional electric power needed to circulate the coolant (i.e. pumping power). In principle, this quantity is different between HTS and Al bus bars due to the different thermodynamic conditions of the employed fluids, and cannot be estimated without a detailed design of the hydraulic circuit.

## 4. Results and discussion

### 4.1. Bus bar design

Hereinafter, we consider two possible bus bar designs, i.e. one with  $I_{op} = 66$  kA, which is the foreseen TF coil current for the European DEMO [18,19] and close to the corresponding value used in ITER [17], and a second one with  $I_{op} = 105$  kA.

We take PA1212 second-generation REBCO tapes supplied by Shanghai Superconductor Technology Co. Ltd., China (see Fig. A2 in Appendix for the critical current performance), with width  $w = 4$  mm and thickness  $t = 0.1$  mm [26]. Four different outer radii of the flexible former are studied, i.e. 25.0, 40.0, 55.0 and 70.0 mm. In addition, we consider three possible operating temperatures, i.e. 50 and 65 K if He gas is available in the cryo-plant, and 77.5 K, in the case of LN<sub>2</sub> cooling.

Following the procedure described above, we obtain a total number of twelve possible bus bar designs for each  $I_{op}$  value. In Tables 1 and 2 we list the proposed 66 and 105 kA bus bar designs, respectively, where with  $B$  we denote the value of the magnetic field extracted from the graphical procedure (see Fig. A1 in Appendix). The number of layers is chosen in order to operate the tapes at around 80% of the critical current.

A larger outer radius of the flexible former allows a cost-effective solution, because it takes advantage of a reduced self-field, thus a smaller number of HTS tapes is required. In addition, a smaller  $N$  would

**Table 3**

66 and 105 kA Al bus bar design, including bus bar weigh per unit length, based on four possible current densities.

$I_{op} = 66$ kA		$J_{Al} = 0.25$ A mm <sup>-2</sup>	$J_{Al} = 0.50$ A mm <sup>-2</sup>	$J_{Al} = 1.00$ A mm <sup>-2</sup>	$J_{Al} = 2.00$ A mm <sup>-2</sup>
$A_{Al}$	mm <sup>2</sup>	264,000	132,000	66,000	33,000
$d_{Al} A_{Al}$	kg m <sup>-1</sup>	713	356	178	89
$I_{op} = 105$ kA		$J_{Al} = 0.25$ A mm <sup>-2</sup>	$J_{Al} = 0.50$ A mm <sup>-2</sup>	$J_{Al} = 1.00$ A mm <sup>-2</sup>	$J_{Al} = 2.00$ A mm <sup>-2</sup>
$A_{Al}$	mm <sup>2</sup>	420,000	210,000	105,000	52,500
$d_{Al} A_{Al}$	kg m <sup>-1</sup>	1134	567	284	142

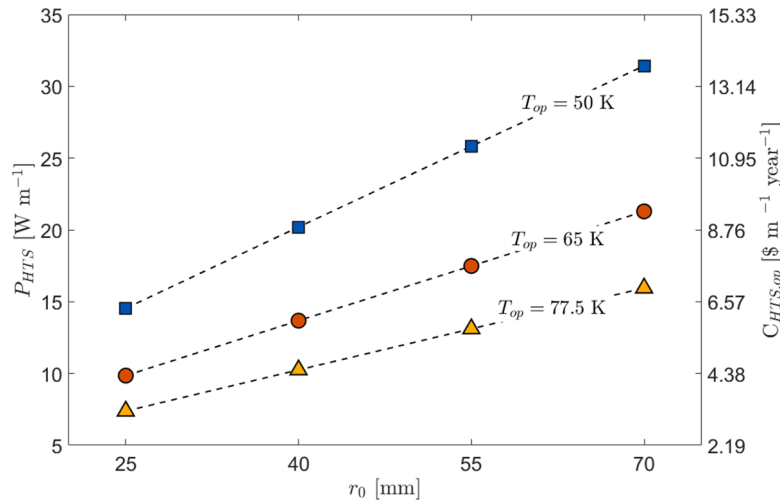


**Fig. 2.** Total room-temperature cooling power required for HTS bus bars, and corresponding yearly operating costs, for different values of  $r_o$  and  $T_{op}$ . Note that we have subtracted the maintenance costs, according to Eq. (13a), in order to show only the cooling costs.

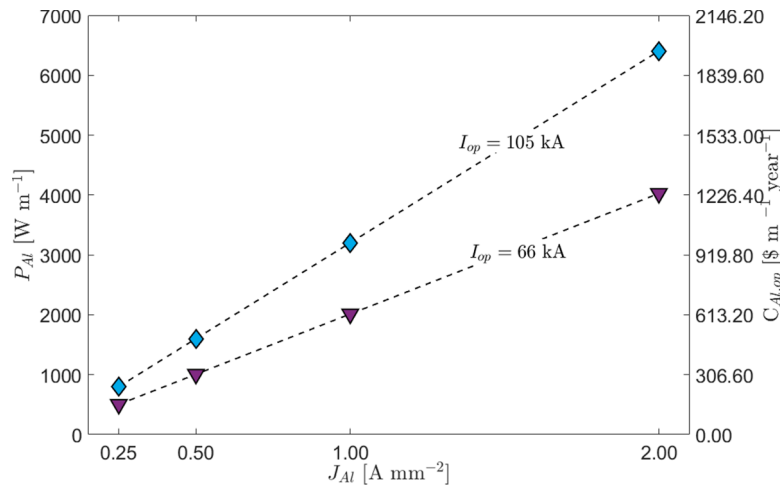


**Fig. 3.** Total electric power losses due to Joule heating of the Al bus bars, and corresponding yearly operating costs, for different values of  $J_{Al}$  and  $I_{op}$ .

potentially reduce also the manufacturing costs and complexity. On the other side, the maximum value of  $r_o$  is limited by the minimum bending radius of the bus bar, which depends on the properties of the flexible stainless steel former, as well as on the tolerable bending radius of the HTS tapes. For conventional conductors with a rectangular cross section, the minimum bending radius is in the range 3 to 6 times the length of the longer side.

The 66 and 105 kA Al-based bus bar designs, instead, are reported in Table 3. In this case, four possible Al current densities  $J_{Al}$  are considered, i.e. 0.25, 0.50, 1.00 and 2.00 A mm<sup>-2</sup>. The unit weight is computed with a material density  $d_{Al} = 2700$  kg m<sup>-3</sup>. We assume a constant electrical resistivity  $\rho_{Al} \approx 3.05 \cdot 10^{-8}$   $\Omega$  m at 60 °C.

#### 4.2. Cooling power

Fig. 2 displays the room-temperature cooling power needed for the HTS bus bars, according to Eq. (5), for different values of  $r_o$  and  $T_{op}$ . We use a 20 mm-thick thermal insulation, starting at the radius  $r_{th,i} = r_o + 5$  mm. This guarantees a sufficiently large gap for hosting the HTS tapes for both considered operating currents (i.e. 66 and 105 kA), thus making the calculation of  $P_{HTS}$  independent from  $I_{op}$ . We also assume  $k = 0.0002$  W m<sup>-1</sup> K<sup>-1</sup> and  $\eta \approx 0.20$  [25]. The total room-temperature cooling power falls in the range 7–32 W m<sup>-1</sup> and has no significant impact on the overall economic feasibility. In practice, the choice of the optimal HTS design can be taken independently from the value of the required

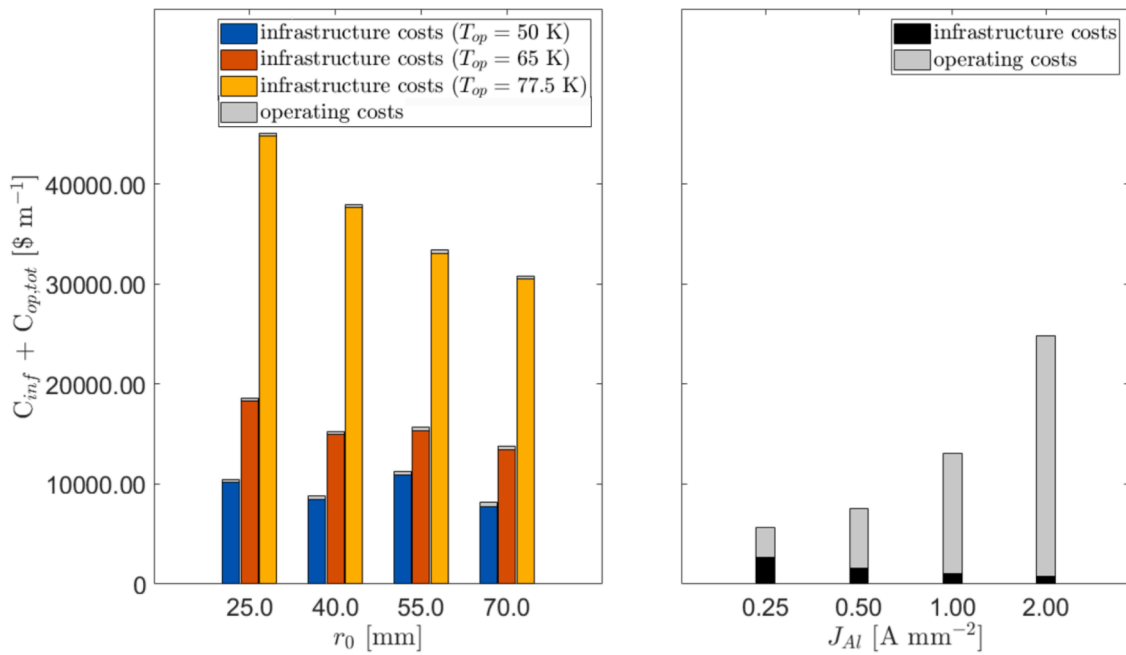


Fig. 4. Cumulative discounted cash flow, over a period of 30 years, for the 66 kA HTS bus bar (left), compared with the solution employing a conventional conductor (right).

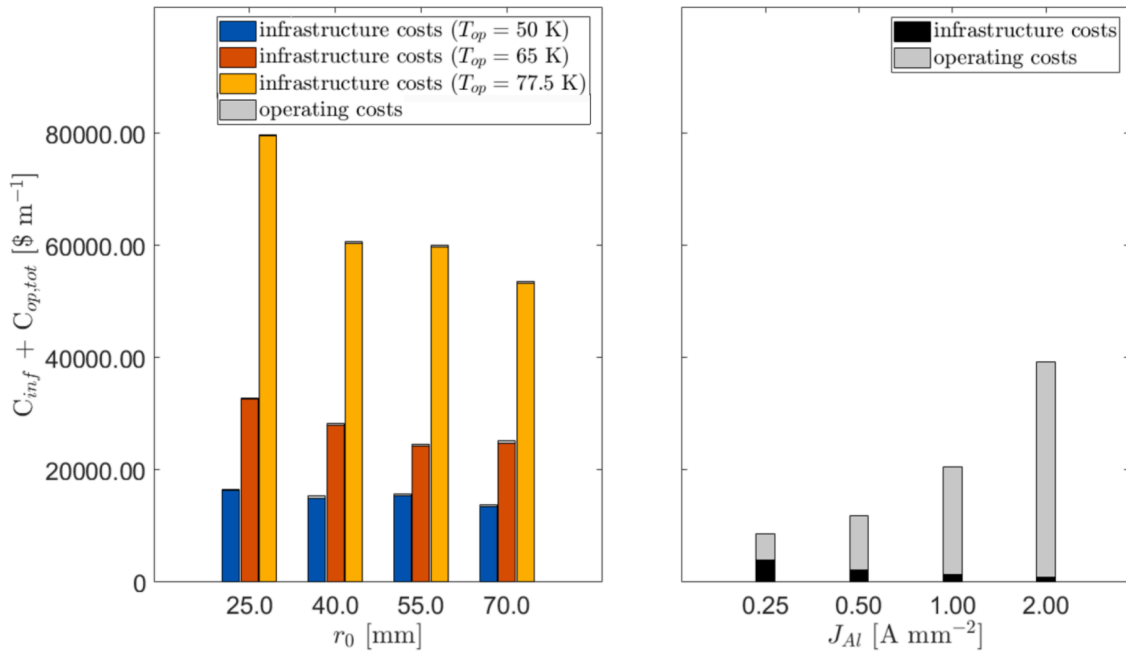


Fig. 5. Cumulative discounted cash flow, over a period of 30 years, for the 105 kA HTS bus bar (left), compared with the solution employing a conventional conductor (right).

cooling power, based on the sole optimisation of the infrastructure costs (as defined above). In general, cooling with He gas supports larger current densities [27], i.e. a smaller  $T_{op}$  allows to reduce the required total number of HTS tapes, at the price of a slightly larger cooling power.

As shown in Fig. 3, the electric power losses due to Joule heating of the Al bus bars is two orders of magnitude larger than  $P_{HTS}$  and goes from 503 (for  $J_{Al} = 0.25 A mm^{-2}$ ) to 4026  $W m^{-1}$  (for  $J_{Al} = 2.00 A mm^{-2}$ ). As will be clear from the cost analysis discussed later, there is a trade-off between a large current density, which allows reduced bus bar dimensions and weights, and a small cooling power, which directly affects the operating costs.

#### 4.3. Cost estimation

For the estimation of the material costs, we assume  $C_{HTS} = 30.00 \$ m^{-1}$  in Eq. (8) [16] and  $C_{Al} = 3.00 \$ kg^{-1}$  in Eq. (10). For the manufacturing costs, following a conservative approach, we assume that the HTS bus bars require four times the manufacturing costs per unit length of the Al bus bars, i.e.  $C_{HTS,mfg} = 2000.00 \$ m^{-1}$  and  $C_{Al,mfg} = 500.00 \$ m^{-1}$ .

The operating costs have been already shown in Figs. 2 and 3 above, where we have assumed an electricity price  $e = 0.05 \$ kWh^{-1}$ . The employed duty cycle is 70% (i.e. 6132  $h year^{-1}$ ) for Al and 95% (i.e.

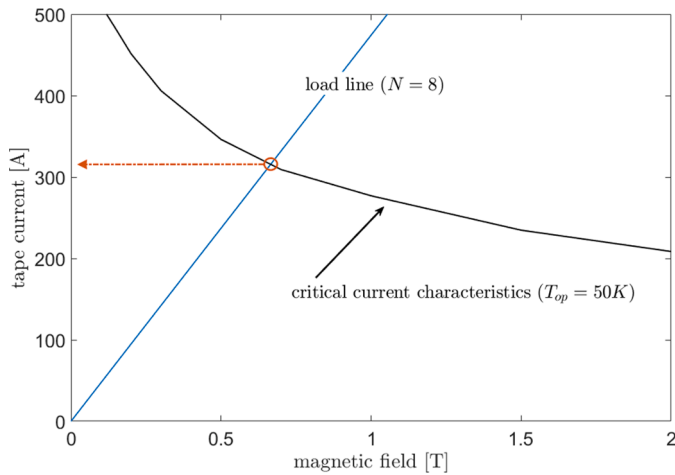


**Fig. A1.** Graphical procedure for the determination of the HTS tape critical current according to Eq. (2). Example case for the tapes considered in Fig. A2, with  $r_o = 25.0$  mm,  $N = 8$  and  $T_{op} = 50$  K. The intersection of the two curves gives  $I_{c,tape} \approx 315.8$  A and, from Eq. (3),  $I_c \approx 85.9$  kA.

8322 h year<sup>-1</sup>) for HTS bus bars, and we have assumed  $C_{HTS,mtt} = 10$  \$ m<sup>-1</sup> year<sup>-1</sup> as an order-of-magnitude estimation.

As mentioned above, each yearly operating cost is discounted according to Eq. (12), assuming an inflation rate  $p = 1\%$  and a discount rate  $q = 4\%$  equal to the weighted average cost of capital [28]. Figs. 4 and 5 display the cumulative discounted cash flows over a period of 30 years, for the 66 and 105 kA bus bars, respectively.

We must specify that an Al bus bar with an extremely low current density, e.g.  $J_{Al} = 0.25$  A mm<sup>-2</sup> as considered in this work, represents always the most favourable solution from the economic point of view. However, its technical feasibility can be questioned, especially if considering the corresponding large unit weight (see Table 3).

As expected, we observe that, in general, a larger outer radius of the flexible former and a lower operating temperature make the HTS solution competitive with respect to Al bus bars. Considering a reasonable Al current density of 1.00 A mm<sup>-2</sup> for the 66 kA bus bar, an HTS design operated at 50 K is always more convenient, while only a large  $r_o$  would allow a cost-effective operation at 65 K. If considering the same reference Al current density for the 105 kA bus bar, instead, no cost-effective HTS operations at 65 K are possible, but a 50 K He gas cooling would be

required.

From Figs. 4 and 5, we note also that an LN<sub>2</sub> cooling (i.e. operating the HTS bus bar at 77.5 K) is never convenient for the considered values of  $r_o$ . Only if a very large outer radius of the flexible former is employed, e.g. in the range  $r_o \geq 100$  mm, could bring slight economic benefits, but at the price of larger minimum bending radii and thus a more complex logistics and integration.

Note that in the example case of the 68 kA DC bus bar for ITER, the proposed Al current density of 2.00 A mm<sup>-2</sup> makes an alternative HTS design absolutely convenient from the economic point of view, even with an operating temperature of 65 K.

### 5. Conclusions

Is it convenient, from a technical and economic point of view, to substitute conventional power conductors with HTS bus bars? In the past decades, this question has had, almost always, a negative answer due to the excessive cost of HTS tapes. In a few exceptional cases, conventional cables have been replaced with HTS ones, but almost exclusively in order to solve technical issues and challenges, rather than for an economic convenience.

However, in the last few years the quick reduction in HTS material costs has changed this scenario and may support the use of HTS cables where they were prohibitively expensive before. In this study, we have taken high-current DC bus bars as reference case for a comparison between Al and HTS technologies.

Our feasibility study indicates that the optimal configuration of HTS and Al bus bars require a compromise amongst several quantities:

- larger outer radii of the flexible former allow to reduce the number of layers, thus reducing HTS costs and manufacturing complexity, at the price of larger minimum bending radii, which must be evaluated case by case;
- lower operating temperatures increase the critical current of HTS tapes, thus reducing the HTS material cost because of a smaller required number of tapes;
- larger Al current densities allow to reduce the unit weight of the cables, at the price of larger electric power losses due to Joule heating.

With reasonable assumptions and focusing on the ranges 50–77.5 K for  $T_{op}$  and 25.0–70.0 mm for  $r_o$ , we have shown that several

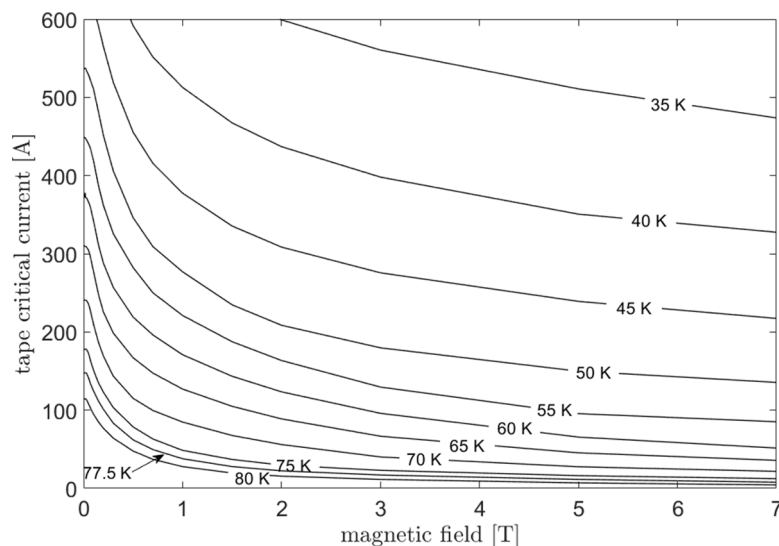


**Fig. A2.** Critical current of the PA1212 second-generation REBCO tapes (Shanghai Superconductor Technology Co. Ltd., China) as function of the magnetic field parallel to the broad face of the tapes, in the temperature range 35–80 K [26].

configurations make the HTS solution more cost-efficient than the corresponding Al bus bars. This result is even more important if we consider that very small Al current densities (i.e.  $J_{Al} = 0.25$  and  $0.50 \text{ A mm}^{-2}$  in Figs. 4 and 5) are not realistic options for a technical point of view, for manufacturing, integration as well as logistics reasons. The trend of price increase in raw materials, furthermore, could represent an additional disadvantage of conventional bus bars.

If lower He gas temperatures would be available (e.g. 20 or 40 K), the situation greatly improves in favour of HTS bus bars, which can be realised with smaller cross-sections. Such a value of  $T_{op}$  would be not difficult to derive in fusion reactors, where several (e.g. warm return) cryo-lines from the superconducting magnets are generally available.

From our feasibility study, even using several conservative assumptions, it is evident that HTS power cables have a great potential from the economic point of view. A realistic reduction in the material cost (from the assumed  $30 \text{ \$ m}^{-1}$ ) in the coming years [16], makes the HTS solution the most convenient way of powering future fusion reactors.

### CRedit authorship contribution statement

**Roberto Guarino:** Conceptualization, Methodology, Formal analysis, Investigation, Writing – original draft, Visualization. **Rainer Wesche:** Conceptualization, Methodology, Validation. **Kamil Sedlak:** Supervision, Funding acquisition.

### Declaration of Competing Interest

The authors declare that they have no known competing financial interests or personal relationships that could have appeared to influence the work reported in this paper.

### Acknowledgement

The authors acknowledge Dr. Davide Uglietti for discussions and the technical support of the Paul Scherrer Institute (PSI).

This work has been carried out within the framework of the EURO-fusion Consortium and has received funding from the Euratom research and training programme 2014–2018 and 2019–2020 under grant agreement No 633053. The views and opinions expressed herein do not necessarily reflect those of the European Commission.

### Appendix. – HTS tapes

Figs. A1 and A2.

### References

- [1] D.W.A. Willén, F. Hansen, C.N. Rasmussen, M. Däumling, O.E. Schuppach, E. Hansen, O.E. Baerentzen, B. Sværre-Hansen, C. Træholt, S.K. Olsen, C. Rasmussen, E. Veje, K.H. Jensen, O. Tønnesen, J. Østergaard, S.D. Mikkelsen, J. Mortensen, M. Dam-Andersen, Test results of full-scale HTS cable models and plans for a 36 kV, 2 kA/sub rms/utility demonstration, *IEEE Trans. Appl. Supercond.* 11 (2001) 2473–2476.
- [2] D.W.A. Willén, F. Hansen, M. Däumling, C.N. Rasmussen, J. Østergaard, C. Træholt, E. Veje, O. Tønnesen, K.H. Jensen, S.K. Olsen, C. Rasmussen, E. Hansen, O.E. Schuppach, T. Visler, S. Kvorning, J. Schuzster, J. Mortensen, J. Christiansen, S.D. Mikkelsen, First operation experiences from a 30 kV, 104 MVA HTS power cable installed in a utility substation, *Phys. C* 372–376 (2002) 1571–1579.
- [3] Y. Xin, B. Hou, Y. Bi, K. Cao, Y. Zhang, S. Wu, H. Ding, G. Wang, Q. Liu, Z. Han, China's 30 m, 35 kV/2 kA ac HTS power cable project, *Supercond. Sci. Technol.* 17 (2004) S332.
- [4] Y. Xin, B. Hou, Y. Bi, H. Xi, Y. Zhang, A. Ren, X. Yang, Z. Han, S. Wu, H. Ding, Introduction of China's first live grid installed HTS power cable system, *IEEE Trans. Appl. Supercond.* 15 (2005) 1814–1817.
- [5] C.S. Weber, C.T. Reis, A. Dada, T. Masuda, J. Moscovic, Overview of the underground 34.5kV HTS power cable program in Albany, NY, *IEEE Trans. Appl. Supercond.* 15 (2005) 1793–1797.
- [6] S. Mukoyama, M. Yagi, M. Ichikawa, S. Torii, T. Takahashi, H. Suzuki, K. Yasuda, Experimental results of a 500m HTS power cable field test, *IEEE Trans. Appl. Supercond.* 17 (2007) 1680–1683.
- [7] L.Y. Xiao, S.T. Dai, Y.B. Lin, Z.Y. Gao, F.Y. Zhang, X. Xu, L.Z. Lin, Development of HTS AC power transmission cables, *IEEE Trans. Appl. Supercond.* 17 (2007) 1652–1655.
- [8] J.F. Maguire, J. Yuan, W. Romanosky, F. Schmidt, R. Soika, S. Bratt, F. Durand, C. King, J. McNamara, T.E. Welsh, Progress and status of a 2G HTS power cable to be installed in the Long Island Power Authority (LIPA) grid, *IEEE Trans. Appl. Supercond.* 21 (2011) 961–966.
- [9] E.P. Volkov, V.S. Vysotsky, V.P. Firsov, First Russian long length HTS power cable, *Phys. C* 482 (2012) 87–91.
- [10] M. Stemmler, F. Merschel, M. Noe, A. Hobl, AmpaCity - Installation of advanced superconducting 10 kV system in city center replaces conventional 110 kV cables, in: Proceedings of 2013 IEEE International Conference on Applied Superconductivity and Electromagnetic Devices, Beijing, China, 2013, 25–27 October.
- [11] S.J. Lee, M. Park, I.K. Yu, Y. Won, Y. Kwak, C. Lee, Recent status and progress on HTS cables for AC and DC power transmission in Korea, *IEEE Trans. Appl. Supercond.* 28 (2018) 1–5.
- [12] S.P. Ashworth, P. Metra, R.J. Slaughter, A techno-economic design study of high-temperature superconducting power transmission cables, *Eur. Trans. Electr. Power* 4 (1994) 293–300.
- [13] M. Runde, Application of high-Tc superconductors in aluminum electrolysis plants, *IEEE Trans. Appl. Supercond.* 5 (1995) 813–816.
- [14] D. Politano, M. Sjöström, G. Schnyder, J. Rhyner, Technical and economical assessment of HTS cables, *IEEE Trans. Appl. Supercond.* 11 (2001) 2477–2480.
- [15] L. Ren, Y. Tang, J. Shi, L. Li, J. Li, S.C. Cheng, Techno-economic feasibility study on HTS power cables, *IEEE Trans. Appl. Supercond.* 19 (2009) 1774–1777.
- [16] D. Uglietti, A review of commercial high temperature superconducting materials for large magnets: from wires and tapes to cables and conductors, *Supercond. Sci. Technol.* 32 (2019), 053001.
- [17] N. Mitchell, A. Devred, P. Libeyre, B. Lim, F. Savary, The ITER magnets: design and construction status, *IEEE Trans. Appl. Supercond.* 22 (2012), 4200809.
- [18] K. Sedlak, V.A. Anvar, N. Bagrets, M.E. Biancolini, R. Bonifetto, F. Bonne, D. Boso, A. Brighenti, P. Bruzzone, G. Celentano, A. Chiappa, V. D'Auria, M. Dan, P. Decool, A. della Corte, A. Dembkowska, O. Dicuonzo, I. Duran, M. Eisterer, A. Ferro, C. Fiamozzi Zignani, W.H. Fietz, C. Frittitta, E. Gaio, L. Giannini, F. Giorgetti, F. Gömöry, X. Granados, R. Guarino, R. Heller, C. Hoa, I. Ivashov, G. Jiolat, M. Jirsa, B. Jose, R. Kembleton, M. Kumar, B. Lacroix, Q. Le Coz, M. Lewandowska, A. Maistrello, N. Misiara, L. Morici, L. Muzzi, S. Nicollet, A. Nijhuis, F. Nunio, C. Portafaix, G. Romanelli, X. Sarasola, L. Savoldi, B. Stepanov, I. Tiseanu, G. Tomassetti, A. Torre, S. Turtù, D. Uglietti, R. Vallcorba, L. Viererbl, M. Wojcniak, C. Vorpahl, K.P. Weiss, R. Wesche, M.J. Wolf, L. Zani, R. Zanino, A. Zappatore, V. Corato, Advance in the conceptual design of the European DEMO magnet system, *Supercond. Sci. Technol.* 33 (2019), 044013.
- [19] R. Guarino, R. Wesche, X. Sarasola, K. Sedlak, P. Bruzzone, A design proposal for the European DEMO superconducting bus bars and current leads, *Fusion Eng. Des.* 169 (2021), 112430.
- [20] A. Sakasai, S. Ishida, M. Matsukawa, G. Kurita, N. Ino, T. Ando, T. Ami, H. Ichige, A. Kaminaga, T. Kato, K. Kim, K. Masaki, Y.M. Miura, Y. Miyo, A. Morioka, S. Sakurai, T. Sasajima, S. Takeji, H. Tamai, K. Tsuchiya, K. Urata, J. Yagyu, K. Tobita, H. Takenaga, K. Shimizu, M. Kikuchi, Engineering design study of JT-60 superconducting modification, in: Proceedings of the 19th IEEE/IPSS Symposium on Fusion Engineering (SOFE), 2002, pp. 221–225.
- [21] R. Wesche, X. Sarasola, R. Guarino, K. Sedlak, P. Bruzzone, Parametric study of the TF coil design for the European DEMO, *Fusion Eng. Des.* 164 (2021), 112217.
- [22] F. Milani, J. Chiron, A. Roshal, V. Lokiev, R. Enikeev, DC busbars for the ITER power supply system: features and challenges, in: IEEE 26th Symposium on Fusion Engineering (SOFE), 2015, pp. 1–6.
- [23] S. Elschner, J. Brand, W. Goldacker, M. Hollik, A. Kudymow, S. Strauss, V. Zermeno, C. Hanebeck, S. Huwer, W. Reiser, M. Noe, 3S - superconducting DC-busbar for high current applications, *IEEE Trans. Appl. Supercond.* 28 (2018), 4800805.
- [24] V.E. Sytnikov, P.I. Dolgosheev, G.G. Svalov, N.V. Polyakova, The magnetic field distribution in the multilayer power superconducting cables, in: EUCAS European Conference on Applied Superconductivity 1999, Sitges, Spain, 1999, 14–17 September.
- [25] R. Wesche, A. Anghel, B. Jakob, G. Pasztor, R. Schindler, G. Vécsey, Design of superconducting power cables, *Cryogenics* 39 (1999) 767–775.
- [26] S. Wimbush, N. Strickland, Critical current characterisation of Shanghai Superconductor PA1212 2G HTS superconducting wire, figshare dataset (2017), <https://doi.org/10.6084/m9.figshare.5331145.v2>.
- [27] S. Pamidi, C.H. Kim, L. Graber, High-temperature superconducting (HTS) power cables cooled by helium gas. Superconductors in the Power Grid, Elsevier, 2015.
- [28] Weighted average cost of capital (WACC) - calculatory interest rate in accordance with Article 13, paragraph 3b, Electricity Supply Ordinance, Swiss Federal Office of Energy (2021) <https://www.bfe.admin.ch/bfe/en/home/supply/electricity-supply/federal-electricity-supply-act/wacc.html>.